Aggregation of a Benzoporphyrin Derivative in Water/Organic Solvent Mixtures: A Mechanistic Proposition

Fernanda Ibanez Simplicio, Rafael Ribeiro da Silva Soares, Florângela Maionchi, Ourides Santin Filho, and Noboru Hioka*

Departamento de Química, Universidade Estadual de Maringá, Avenida Colombo, 5790, 87020-900 Maringá, Paraná, Brazil

Received: April 2, 2004; In Final Form: August 6, 2004

The kinetics of the aggregation process of DiesterB, a homologous coproduct generated in Verteporfin synthesis (the drug used in the medication Visudyne applied in photodynamic therapy), was investigated by visible spectrophotometry in several aqueous organic solvents (dimethyl sulfoxide (DMSO), acetonitrile, dioxane, methanol, and ethanol). The monomeric form of DiesterB is stable in pure organic solvents, showing a characteristic peak at 690 nm. In water-rich medium, an aggregation process is induced, giving rise to a new band in the 720−740 nm region. In aqueous DMSO and acetonitrile solvents this process is very fast and leads to the formation of dimers, while in dioxane−, methanol−, and ethanol−water mixtures the absorption intensities show a sigmoidal time profile, suggesting a slow initial reaction (lag phase) followed by a rapid aggregation (log phase), characteristic of autocatalyzed reactions. The proposed final species in these solvents is a trimer as the main aggregate (supported by resonance light scattering and small-angle X-ray scattering experiments). The experimental absorbance values, taken at monomer or aggregate peaks during the reaction, were fitted using a nonconventional treatment proposed by Pasternack. This model allows evaluating two rate constants, due to a first (k_0, noncatalytic) and a second (k_c, catalytic) step, as well as a parameter (m), related to the size and amount of the catalyst nucleus. Although the model was originally applied to large porphyrin arrays growing on templates, an excellent accordance was obtained between its formalism and our kinetic experimental data. The global mechanism seems to start with a dimeric nucleus formation (lag phase), which acts, despite its small amount, as a catalytic center driving to trimers (log phase). The effects caused by water content and DiesterB concentration on the kinetic results support the proposed multistep equilibrium. The absence of isosbestic points during the process reinforces the presence of more than one step. The most unusual feature is the effect of the temperature on the rate constants. As the temperature is raised, the constants increase up to a maximum, and decrease for higher temperatures. The effect is more pronounced for k_c than for the k_0 rate constant. The model proposed states that at high temperatures the equilibrium is shifted toward monomers, reducing the catalyst nucleus formation and resulting in an overall reaction velocity decrease.

Introduction

Photodynamic therapy (PDT) is a medical modality that employs a photosensitizer compound and light to generate reactive species (singlet oxygen), which induces damage to malignant tissues, without serious side effects.[1−3] The latest medication approved for PDT by the Food and Drug Administration (FDA, USA), Visudyne, is applied in over 60 countries to fight macular degeneration of the retina (the major cause of blindness in the elderly).[4] The FDA has evaluated this drug against other diseases such as multiple basal cell tumor (skin cancer) and pathologic myopia.[5,6] This medication contains as active compound a porphyrin derivative, benzoporphyrin monoacid (BPDMA), named Verteporfin, which is applied in liposomal formulation (drug carrier system).[1,6] The synthetic route[3] of BPDMA starts from protoporphyrin IX dimethyl ester, producing two homologous chlorin-like compounds, with one cyclohexadiene ring fused at a reduced pyrrole ring (pyrrole porphyrin ring A and B regioisomers, produced in equimolar quantities). From these compounds, the 1,4-diene system is isomerized to the 1,3-diene system and, using a hindered and strong base, generate a compound with the methyl ester moiety positioned transoid to the methyl group, yielding a tetraester product (that we named DiesterA and DiesterB photosensitizers). BPDMA (9-methyl(I) and 13-methyl(II) *trans*-(±)-18-ethenyl-4,4a-dihydro-3,4-bis(methoxycarbonyl)-4a,8,14,19-tetramethyl-23*H*,25*H*-benzo[*b*]porphine-9,13-dipropanoate) is produced from controlled acid hydrolysis of DiesterA.

Despite its structural similarity and efficiency for PDT uses, the B-ring derivatives (DiesterB and its monoacid form, generated as 1:1 coproduct), have shown a much higher tendency to undergo autoaggregation in water than A-ring compounds.[7,8] The aggregation phenomena are frequently observed in porphyrin compounds in aqueous medium.[9,10] The aggregate state of porphyrin derivatives is inefficient for PDT applications due to its low singlet oxygen yield (species responsible for the local damage), which reduces the therapeutic potentialities.[3,11−13]

Based on thermodynamic aspects, our research group has proposed that the process of DiesterB aggregation is a complex subject. Studies on aggregation of this compound in water/dimethyl sulfoxide (DMSO) and in water/acetonitrile[14,15] pointed out that dimers are the main aggregates, while in water with

* To whom correspondence should be addressed. E-mail: nhioka@uem.br.

10.1021/jp048542g CCC: $27.50
Published on Web 09/28/2004

dioxane, methanol, and ethanol, trimer is proposed as the predominant form.[15]

The aim of the present work is to clarify the dependence of the aggregation kinetics of DiesterB on the water content in organic solvents, as well as on the concentration of DiesterB and the temperature, in order to elucidate the mechanism of this aggregation, which process is not beneficial for PDT application.

Experimental Section

Materials and Methods. DiesterB, kindly supplied by professor David Dolphin (University of British Columbia, Vancouver, BC, Canada), was synthesized in accord with the described method.[3,16] All solvents employed (DMSO, Mallinckrodt; acetonitrile, Mallinckrodt; 1,4-dioxane, Merck; methanol, Aldrich; and ethanol, Merck) were of analytical grade. Deionized, doubly distilled water in an all-glass apparatus was used throughout. Standardized DiesterB solution, prepared in DMSO (molar absorptivity $\epsilon = 34\,000$ L mol^{-1} cm^{-1} at 690 nm [14]), was kept frozen in the dark. The water composition in the organic solvent was taken by water percentage in volume (final volume obtained in a volumetric flask). We consider that the small volume change due to the mixture of water/organic solvents does not interfere with the results, and its effects are overwhelmed by those brought by the final physicochemical properties of the solvent mixtures. The solvent mixture was thermally stabilized in the spectrophotometer cell, and the porphyrin was introduced by a microsyringe followed by a vigorous shaking of the sample (mechanical plate mixer for 10 s). The aggregation process was followed by absorbance changes at 690 nm (Q-band of the monomer peak), at 430 nm (Soret band of the monomer peak), and in the 720−740 nm region (aggregate band) under controlled temperature. Kinetic parameters were obtained from curve fitting to eq 1 (see below) with the software KaleidaGraph[17] using more than 600 data points. The aggregation was also followed by fluorescence spectrophotometry at 430 nm (excitation) and 699 nm (emission) wavelengths, in diluted solution ($Abs_{430\,nm} < 0.1$).

Equipment. The experiments were performed in Cary-50 (Varian) and DU-70 (Beckman) spectrophotometers, using quartz or polystyrene cuvettes with 1.00 cm optical paths. The spectrofluorometer was a SPEX Model DM3000F equipped with a 150 W xenon lamp; excitation and emission slits were kept at 1 mm (band-pass 13 nm). For resonance light scattering (RLS) measurements the spectrofluorometer was a SPEX Model 1681 Fluorolog with a 150 W xenon Lamp, with detection at 90° relative to excitation. The excitation and emission monochromator wavelengths were coupled and adjusted to scan simultaneously from 300 to 800 nm (synchronous scanning mode). [DiesterB] $= 3 \times 10^{-6}$ mol L^{-1} in 60% water in ethanol. Both fluorometers were used at Instituto de Quimica—USP, Brazil). Small-angle X-ray scattering (SAXS) experiments were executed at the National Synchrotron Light Laboratory (LNLS) in Campinas, Brazil, in a 2 mmol/L solution of DiesterB in 50% water in ethanol. The radiation wavelength was 1.608 Å with a sample-to-detector distance of 600 mm at room temperature (24 ± 1 °C). Samples were kept in sealed 1 mm thick acrylic cells, with mica windows, perpendicular to the incident X-ray beam. Conventional treatment was applied to the raw data, such as normalization and subtraction of incoherent noise.

Kinetic Treatment. The curves observed in the aggregation process of DiesterB were analyzed by a nonconventional kinetic treatment, proposed by Pasternack,[18,19] who investigated several systems involving spontaneous aggregation phenomena, mainly porphyrin arrays (assembly) on biopolymers (as templates). Contrary to classical kinetic treatment, this nonconventional model states that some rate constants show time dependence.[20,21] The mathematical model considers that some catalytic centers (nuclei or "seeds") are formed as an initial step, a "delay period". Once they are formed, these nuclei catalyze the subsequent aggregation process forming a final porphyrin array with higher aggregation number−growth phase. This first (nucleation) step, characterized by k_0, a noncatalytic and time-independent rate constant, is the "bottleneck" of the array formation. After this first step, the reactivity increases as a function of time, which step is associated with k_c, a time-dependent, catalytic rate constant. Based on fractal aggregate, this rate constant is proportional to the mean size, $s(t)$, which increases with a power-law dependence on time:

$$k_c \propto s(t) = t^n$$

where n is related to the growing rate of the catalyzed array. The overall rate constant, $k(t)$, can be written as

$$k(t) = k_0 + k_c(k_c t)^n$$

(association of the noncatalytic and the catalytic steps).

The rate law for the dependence of the monomer (M) concentration can be expressed as

$$-(\mathrm{d}[\mathrm{M}]/\mathrm{d}t) \propto \{[\mathrm{M}] - [\mathrm{M}_i]\}^m$$

where [M] and [M_i] are the monomer concentration at a given time and at equilibrium, respectively. According to the authors the m parameter is related uniquely to the nucleus size (see Discussion). The fractal-like systems can produce anomalous reaction orders, so its value may depend on the initial experimental conditions.

Following the statements of Pasternack, the kinetic data can be fitted using a closed-form integrated rate law represented by eq 1, involving four kinetic parameters (k_0, k_c, m, and n).

$$(\mathrm{Abs} - \mathrm{Abs_{inf}})/(\mathrm{Abs_0} - \mathrm{Abs_{inf}}) = 1/(1+(m-1)[k_0 t + (n+1)^{-1}(k_c t)^{n+1}])^{1/(m-1)} \quad (1)$$

where Abs, Abs_{inf}, and Abs_0 are the absorbance values at a given time, at infinity, and at the initial time, respectively. In the fitting routine, we take Abs_{inf} and Abs_0 as additional calculated parameters, so they were compared directly to our experimental results. The m and n parameters were considered variable, and their physical meaning may not be quite so straightforward.

Results

The electronic absorption spectrum of DiesterB in pure DMSO, acetonitrile, dioxane, methanol, and ethanol showed an intense Soret band at 430 nm (characteristic to porphyrin molecules) and a main Q-band at 690 nm with moderate intensity (characteristic of chlorin structures); these peaks correspond to monomer in solution. The presence of water in these organic solvents reduces the intensity of the monomer peaks (690 and 430 nm) while a new band, due to aggregate formation, shows up in the 720−740 nm region. This process in water/DMSO and water/acetonitrile systems occurred immediately after DiesterB addition (too fast to be followed by the conventional methods employed), while in aqueous dioxane, methanol, and ethanol the spectra exhibited a gradual decreasing of the monomer peak, together with an increasing aggregate

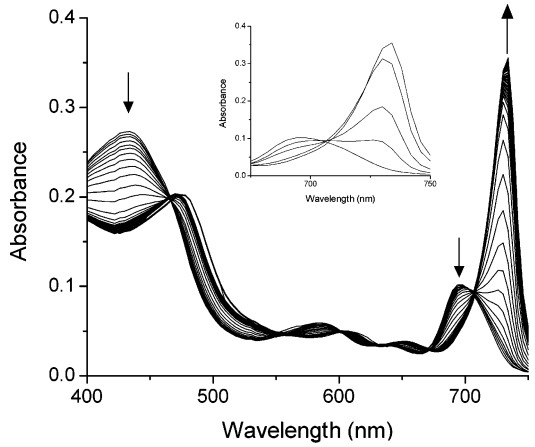

Figure 1. Successive spectra of the DiesterB (5.07×10^{-6} mol L^{-1}) aggregation process in 50% water in methanol. $T = 30.0$ °C; time step = 12 s (total time 20 min). Inset: time step = 48 s.

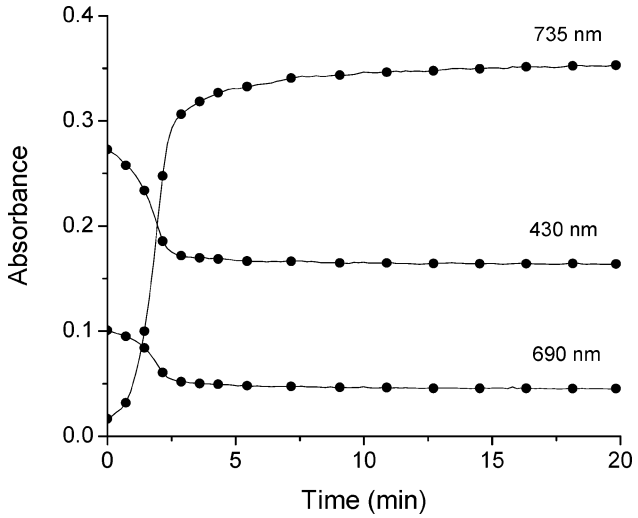

Figure 2. Kinetic behavior of the absorbance for DiesterB ($c = 3.20 \times 10^{-6}$ mol L^{-1}) in 50% water in methanol. $T = 30.0$ °C.

band. The final equilibrium was reached in 20 min (see Figure 1 for water/methanol system as example).

The spectral sequence in Figure 1 (water/methanol) seems to show an isosbestic point around 707 nm, but the enlargement of the scale (inset in Figure 1) shows that this point is quasi-isosbestic. Such a point was not observed for aqueous solvent mixtures of dioxane and ethanol.

The monomer and aggregate peak absorption intensities, as a function of time, are presented in Figure 2.

As can be seen, the reaction exhibits the same kinetic feature at the monomer (430 and 690 nm) and aggregate (735 nm) peaks, beginning with a slow period followed by a rapid change to the final equilibrium (absorption intensity at infinity).

Attempts to model the absorbance data against time, to a two-step pathway in which the reactions can correspond to one of the schemes illustrated below (without a catalyzed step),[22] were not successful.

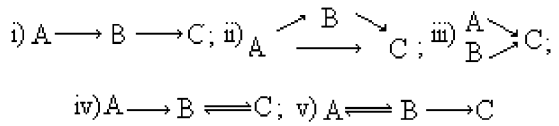

However, the existence of a delay period with the "sigmoidal progress profiles" led us to employ the nonconventional model

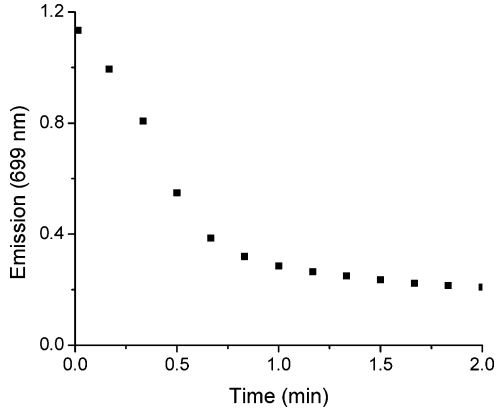

Figure 3. Fluorescence intensity (arbitrary units) as a function of time. [DiesterB] = 6.0×10^{-7} mol L^{-1} in 60% water in ethanol. $T = 35.0$ °C.

TABLE 1: Calculated Kinetic Parameters for DiesterB Aggregation in 50% Water in Methanol[a]

wavelength (nm)	k_0 (min^{-1})	k_c (min^{-1})	m	n
430	0.28	0.80	4.2	12
690	0.25	0.79	4.7	8
735	0.24	0.79	4.8	11

[a] [DiesterB] = 3.20×10^{-6} mol L^{-1}. $T = 30.0$ °C.

proposed by Pasternack. According to this,[20,21] the initial slow step (noncatalytic induction period, represented by k_0) termed the "lag phase", is followed by a rapid step (catalytic, represented by k_c), the "log phase". A very good curve fitting of eq 1 was obtained over the entire data set, as can be seen in Figure 2. Similar results are obtained if one observes the fluorescence of the sample. The monomeric form of porphyrin derivatives shows fluorescence emission, while its aggregate forms are not fluorescent, due to a self-quenching process.[12−14,18,19] This allows following the disappearance of the monomer parallel to the aggregation process (Figure 3).

As observed, the growth of porphyrin array monitored by fluorescence resulted in a time profile very similar to that obtained by absorption techniques, presenting lag and log phases. The calculated kinetic parameters using eq 1 show close accordance between both methods.

The kinetic parameters (k_0, k_c, m, and n) obtained in the three absorption wavelengths used (data in Figure 2) are presented in Table 1 for the system water/methanol.

The data show that the parameters obtained by following the monomer and aggregate peaks are almost identical, except for the n value. This analytical wavelength-independent feature was verified for DiesterB in water with dioxane, methanol, and ethanol systems, so that in this work the data obtained from the aggregate peak were employed. The n parameter varied significantly and was not taken into account (see Discussion).

Effect of Water Content in the Organic Solvent on Aggregation. The kinetic parameters of DiesterB aggregation were investigated for several mixtures of water in dioxane, methanol, and ethanol. The values of m, k_0, and k_c parameters, calculated from the fitting of eq 1 on the aggregate band intensities, are presented in Figure 4 for each water percentage.

As observed in Figure 4, the two constants (k_0 and k_c) are dependent on the water concentration and increase as its content is increased. This effect is more pronounced for k_c than for k_0, with nearly the same behavior for all three solvent systems. For the m parameter, it is almost constant for water/dioxane solvent but changes strongly for water/methanol and water/ethanol mixtures.

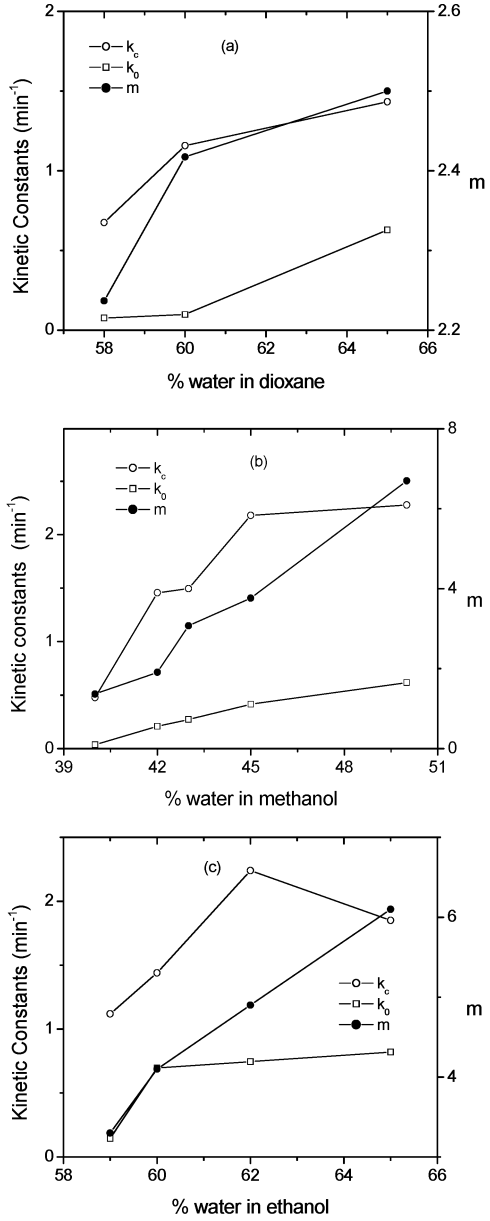

Figure 4. Kinetic parameters at various water/organic solvent mixtures. [DiesterB] = 5.34×10^{-6} mol L^{-1}. T = 30.0 °C. (a) Water/dioxane; (b) water/methanol; (c) water/ethanol.

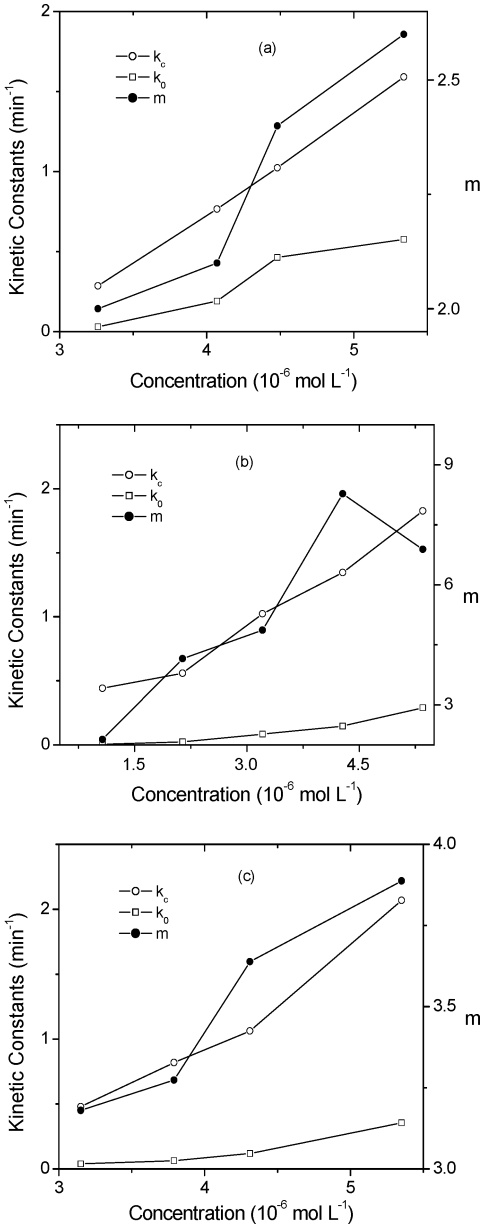

Figure 5. Kinetic parameters as a function of [DiesterB] in (a) 60% water/dioxane, (b) 50% water/methanol, and (c) 60% water/ethanol. T = 30.0 °C.

DiesterB Concentration Effect on Aggregation. The same behavior of the constants is observed when one changes the DiesterB concentration, from 1×10^{-6} to 5×10^{-6} mol L^{-1}, as can be seen in Figure 5, for the systems 60% water/dioxane, 50% water/MeOH, and 60% water/ethanol.

As in the water content effect, the two rate constants increase as a function of DiesterB concentration, but it shows much more influence on k_c than on k_0 for all mixtures. Also the m values increase as [DiesterB] is increased. Once again the water/dioxane system shows the lowest m values.

Temperature Effect on Aggregation. The process of aggregation was studied also as a function of temperature. As illustrated in Figure 6, the behavior of the three parameters is strongly different from those obtained in changing the water and DiesterB concentration. For the three solvent systems, the m parameter decreases as the temperature is raised; the noncatalytic (k_0) rate constant can be taken as almost invariant while the catalytic (k_c) rate constant increases to a maximum and decreases at high temperatures.

Discussion

In previous works,[14,15] thermodynamic studies of aggregation of DiesterB showed that in water/DMSO and water/acetonitrile systems dimers are the predominant aggregates, formed in a single equilibrium between monomers and dimers. Additionally, in both solvent systems, the experiments showed fast kinetics, too fast to be followed by conventional methods. However, in water with dioxane, methanol, and ethanol systems, it seems that the predominant final species is mainly a trimer, in equilibrium with monomers.[15] The fact that one class of solvent produced dimer as final aggregate, as in water/acetonitrile and water/DMSO, and mainly trimer for water/dioxane, water/methanol, and water/ethanol solvent systems, is remarkable. One possibility to account for this difference is to consider the solute−solvent interactions, via the hydrophobic effect, supposing that the former solvents (water with DMSO and acetonitrile) are more efficient in enclosing the solute than the latter ones (water with dioxane, methanol, and ethanol).

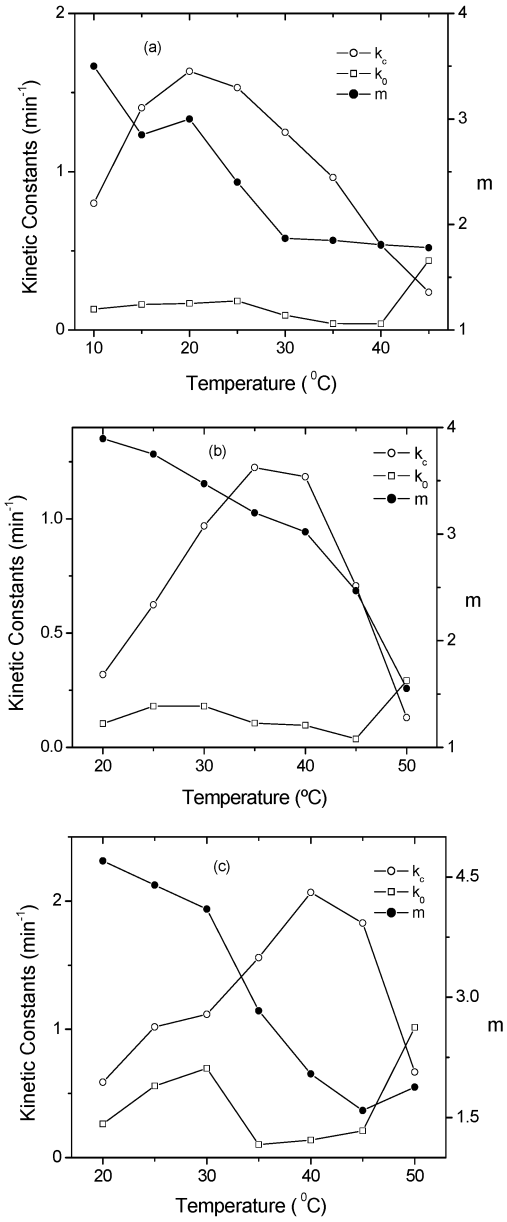

Figure 6. Temperature dependence of calculated kinetics parameters for [DiesterB] = 5.34×10^{-6} mol L^{-1} in (a) 60% water/dioxane, (b) 50% water/methanol, and (c) 60% water/ethanol.

The absence of a clear isosbestic point in the electronic spectra during aggregation (Figure 1) in dioxane, methanol, and ethanol mixtures establishes that the mechanism is rather complex, implying a multistep equilibrium[15,23,24] in these solvents. According to this, we propose a first step, slow reaction of small aggregate formation (in reduced amount), governed by k_0, followed by a rapid, catalyzed, aggregate-growing step (k_c) to produce the final aggregate, which in the present case is mainly trimer.

The aggregation mechanism can be explained considering the initial step, with nucleus generation as intermediate. This is the slow step (lag phase), which we can attribute to formation of small aggregates like dimers. This species can act as catalytic centers, where one additional monomer is catalytically added to the center, forming trimers. Despite generation in small concentration, this nucleus may amplify the velocity to final product. The resulting kinetic curve (Figure 2) is similar to that obtained by our research group with a monoacid BPD-B ring derivative in pluronic acid aqueous systems.[25] These intermediate nuclei, which are generated and consumed during the reaction, were neglected in our previous work,[15] since their presence is unappreciable at final equilibrium. It should be emphasized that, compared with a common two-step equilibrium, we have here all the same chemical species taking part in the global process (monomers, dimers, and trimers); however, the model proposed here supposes a catalytic role for dimers which, once formed, catalyzes a monomer−dimer reaction to form trimers. This proposition is discussed in the present work.

The failed efforts to model the absorption intensity versus time (Figure 2) in the two-step (noncatalyzed) pathway and the sigmoid aspect lead us to use the Pasternack model based on autocatalyzed processes.[26] Although the final aggregates usually cited by that author are porphyrin assemblies (higher arrays) growing in a template,[20,21] instead of dimers and trimers (smaller aggregates), the agreement between the model and the experimental results is striking.

According to Pasternack's model, the n and m parameters are related to the growth rate and size of aggregates.[20,21] In the present investigation, the quality of the fitting does not change when different n values are used in the calculations. In this case, one can admit that the n parameter plays a minor role in the growth rate, as it does in the original model. This characteristic can arise from the fact that, in our system, the aggregate is small (instead of polymeric arrays as investigated by Pasternack). With respect to the m parameter, the values are strongly different from those obtained by Pasternack.[20,21] His original model proposes that this quantity comprises the nucleus size. In this work we have obtained higher values ($2 < m < 8$), so our proposition is that m accounts not only for the nucleus size but also for the quantity of nuclei since even the final aggregates are mainly trimers.[15] It should be stressed that this possibility is also supported by the fact that m values decrease as the temperature is increased.

To solve the question concerning the size of the aggregates, we performed SAXS and RLS experiments in samples where the absorption peak of the aggregate was stabilized (measured 20 min after the DiesterB addition). For the SAXS, no difference was detected between the scattered intensity of the sample and the background, suggesting that the aggregates are too small to be detected by this method. No significant signal was obtained, even for 2 mmol/L DiesterB in 50% water in ethanol solution. Additionally, the RLS experiment showed no scattering signal enhancement, which implies that the absorbing species are limited to small aggregates.[27,28] Both results are in accordance with our proposition.

However, the employed kinetic theory was developed for a supramolecular aggregation process, usually an assembly of porphyrin growing on templates where the catalytic action is explained by a nucleus surface phenomenon. Our basic proposition is that the surface catalytic effect can be exercised by small particles. Additionally, we believe that k_c is not only proportional to the nucleus mean size but also to the quantity of this nucleus, similarly as discussed for the m parameter. In chlorophyll a studies in aqueous solvents (without templates), the Pasternack kinetic treatment was applied; although the minimum aggregation number of the final species was estimated to be 25, the suggested catalytic nucleus was monomers or dimers.[29] In that case the strong hydrophobic effect due to the phytyl chain would play a major role in the process, similar to that occurring in micelles. Additionally, in an investigation[25] of the monoacid BPD-B ring derivative (compound similar to DiesterB) in aqueous Pluronics P123 (a triblock polymer, PEO−PPO−PEO, which shows surfactant properties and can act as template) the

kinetic data exhibited the same sigmoidal profile, suggesting a similarity to our case.

The process of aggregation is affected by the water content and the concentration of DiesterB. In thermodynamic studies,[14,15] this is evidenced by the increase of the equilibrium constants, and in this work, it becomes clear by the kinetics rate constants and by the *m* parameter. For all three solvent systems studied, the slow step seems almost independent of the catalytic centers, as showed by the low dependence of k_0 ($0.1 < k_0 < 0.8$ min^{-1} for all the three systems) on the *m* parameter. On the other hand, in [DiesterB] and water content experiments, the behavior of *m* is reflected in the catalytic constant k_c (as expected) in such a way that as *m* values increase the k_c values increase, which supports the role played by the nuclei as catalytic centers of aggregation.

Additionally, the trend exhibited by *m* and k_c as a function of temperature seems to be divergent. The formation of these nuclei is strongly dependent on the temperature.[15] The value of *m* decreases as the temperature is raised, which implies lower k_c values. However, classically, the reactivity increases as the temperature increases. In our systems, this classical behavior prevails up to a maximum value where it is overcome by the effect of lesser thermodynamic stability of the nuclei, which reduces this quantity and diminishes the global aggregation rate by reducing catalyst concentration. This result strongly reinforces the existence of the nuclei as catalytic intermediates.

The kinetic differences for the DiesterB aggregation in water with DMSO and acetonitrile from water in dioxane, methanol, and ethanol remain obscure. The dependence of the kinetic parameters studied here and the intrinsic properties of the solvents, such as dielectric constant, polarity, polarizability, and protonicity, are under investigation by our research group.

Conclusion

The model applied for the DiesterB aggregation in water/organic solvent mixtures supposes the formation of an intermediate nucleus at small concentration, during the aggregation first step. The rate constant (k_0) of this first step does not depend on the number and size of nuclei formed. In their turn, these species act as catalytic centers, accelerating the overall reaction. Although there are structural differences between Pasternack's model (large aggregates as porphyrins assemble supported over polymeric templates) and our proposition (free dimeric porphyrin nuclei in solution), the model is successfully applied, supporting our proposition of an autocatalyzed reaction (dimers as catalytic nuclei). These dimers can exist in a multistep equilibrium during the aggregate formation (with monomers and trimers which we proposed as the main final species).The proposed mechanism is supported especially by the experiments varying temperature with kinetic parameters. The model can, at last, be expanded to other aggregates.

The aggregation process of DiesterB can be reduced by decreasing the water percentage in the organic solvents or by increasing the temperature. This can be very helpful in drug formulation for topical treatment, since it opens the possibility of using a water-insoluble drug (which proved to be efficient) in photodynamic therapy. The knowledge of the aggregation mechanism, especially the importance of the catalytic centers present in the overall process, would help to develop more stable and efficient medications.

Acknowledgment. This work was supported by the Brazilian granting agencies Fundação Araucária−Paraná and Capes. The authors are grateful to the National Synchrotron Light Laboratory (Campinas) and Rosangela Itri (IF/USP) for the SAXS experiments and Mario J. Politi (IQ/USP) for the fluorescence and RLS experiments.

References and Notes

(1) Sternberg, E. D.; Dolphin, D. *Curr. Med. Chem.* **1996**, *3*, 239.
(2) Levy, J. G. *Tibtech* **1995**, *13*, 14.
(3) Sternberg, E. D.; Dolphin, D.; Brükner, C. *Tetrahedron* **1998**, *54*, 4151.
(4) U.S. Food and Drug Administration. http://www.fda.gov (accessed November 2003).
(5) QLT Inc. http://www.qltinc.com (accessed November 2003).
(6) Oku, N.; Saito, N.; Namba, Y.; Tsukada, H.; Dolphin, D.; Okada, S. *Biol. Pharm. Bull.* **1997**, *20* (6), 670.
(7) Richter, A. M.; Waterfield, E.; Jain, A. K.; Sternberg, E. D.; Dolphin, D.; Levy, J. G. *Photochem. Photobiol.* **1990**, *52*, 495.
(8) Richter, A. M.; Waterfield, E.; Jain, A. K.; Allison, B.; Sternberg, E. D.; Dolphin, D.; Levy, J. G. *Br. J. Cancer* **1991**, *63*, 87.
(9) White, W. I. *The porphyrins*, Dolphin, D., Ed.; Academic Press: New York, 1978; Vol. 3, part C, p 303.
(10) Vladkova, R. *Photochem. Photobiol.* **2000**, *71* (1), 71.
(11) Colussi, V. C.; Feyes, D. K.; Mulvihill, J. W.; Li, Y.; Kenney, M. E.; Elmets, C. A.; Oleinick, N. L.; Mukhtar, H. *Photochem. Photobiol.* **1999**, *69*, 236.
(12) Aveline, B. M.; Hasan, T.; Redmond, R. W. *J. Photochem. Photobiol. B* **1995**, *30*, 161.
(13) Aveline, B. M.; Hasan, T.; Redmond, R. W. *Photochem. Photobiol.* **1994**, *59*, 328.
(14) Delmarre, D.; Hioka, N.; Boch, R.; Sternberg, E. D.; Dolphin, D. *Can. J. Chem.* **2001**, *79*, 1068.
(15) Simplicio, F. I.; Maionchi, F.; Santin Filho, O.; Hioka, N. *J. Phys. Org. Chem.* **2004**, *17* (4), 325.
(16) Sternberg, E. D.; Dolphin, D.; Tovey, A.; Richter, A. M.; Levy, J. G. U.S. Patent 5,880,145, 1999.
(17) *KaleidaGraph*, Demo version 3.51; Synergy Software: Reading, PA, 2000.
(18) Dairou, J.; Vever-Bizet, C.; Brault, D. *Photochem. Photobiol.* **2002**, *75* (3), 229.
(19) Aveline, B.; Redmond, R. W. *Photochem. Photobiol.* **1999**, *69* (3), 306.
(20) Pasternack, R. F.; Gibbs, E. J.; Collings, P. J.; dePaula, J. C.; Turzo, L. C.; Terracina, A. *J. Am. Chem. Soc.* **1998**, *120*, 5873.
(21) Pasternack, R. F.; Ewen, S.; Rao, A.; Meyer, A. S.; Freedman, M. A.; Collings, P. J.; Frey, S. L.; Ranen, M. C.; dePaula, J. C. *Inorg. Chim. Acta* **2001**, *317*, 59.
(22) Moodie, R. B. *J. Chem. Res., Synop.* **1986**, 144.
(23) Espenson, J. H. *Chemical Kinetics and Reactions Mechanism*; McGraw-Hill: New York, 1981; p 117.
(24) Dixon, D. W.; Steullet, V. *J. Inorg. Biochem.* **1998**, *68*, 25.
(25) Hioka, N.; Chowdhary, R. K.; Chansarkar, N.; Delmarre, D.; Sternberg, E. D.; Dolphin, D. *Can. J. Chem.* **2002**, *80*, 1321.
(26) Micali, M.; Scolaro, L. M.; Romeo, A.; Mallamace, F. *Physica A* **1998**, *249*, 501.
(27) Pasternack, R. F.; Bustamante, C.; Collings, P. J.; Giannetto, A.; Gibbs, E. J. *J. Am. Chem. Soc.* **1993**, *115*, 5393.
(28) Pasternack, R. F.; Gurrieri, S.; Lauceri, R.; Purrello, R. *Inorg. Chim. Acta* **1996**, *246*, 7.
(29) Agostiano, A.; Cosma, P.; Trotta, M.; Monsù-Scolaro, L.; Micali, N. *J. Phys. Chem. B* **2002**, *106*, 12820.